UPDATE TO THE USDA-ARS FIXED-WING SPRAY NOZZLE MODELS

B. K. Fritz, W. C. Hoffmann

ABSTRACT. *The current USDA-ARS aerial spray nozzle models were updated to reflect both new standardized measurement methods and systems as well as to increase operational spray pressure, aircraft airspeed, and nozzle orientation angle limits. The new models were developed using both central composite design and custom design response surface methodologies, which provide excellent fits to independently measured data (R^2 values ranging from 0.81 to 0.99) for all droplet size parameters. The new models also updated the droplet size classification ratings by adopting a previously recommended set of nozzles and operational pressures that provide similar data to ASABE Standard Reference nozzles but are evaluated under aerial application conditions (primarily airspeed). Generally, for flat fan and deflection type nozzles, the new models result in increases to predicted $D_{V0.1}$ data (droplet diameter at which 10% of the total spray volume is contained in droplets of equal or lesser diameter), decreases in $D_{V0.5}$ and $D_{V0.9}$ data (similar to $D_{V0.1}$ but 50% and 90% of total spray volume), and increases in the percent of spray contained in droplets of 200 μm diameter or smaller. With straight stream nozzles, the $D_{V0.1}$, $D_{V0.5}$, and $D_{V0.9}$ trends tend to be reversed. Droplet size classifications with the new models for flat fan and deflector type nozzles tend to shift ratings downward, as compared to the current models, with classes centered around fine and medium sprays. However, with straight stream nozzles, droplet size classifications tend to shift ratings upward as compared to the current models. The updated models will be used to populate spreadsheet and mobile device software-based user interfaces to provide aerial applicators with droplet size information for an increased range of nozzles and operational settings, allowing for better nozzle selection and operational guidance.*

Keywords. *Aerial application, Droplet size, Spray droplet size, Spray model, Spray nozzles.*

Spray droplet size has long been recognized as the dominant factor with respect to spray drift, with smaller droplets having a greater tendency to move off the application site than larger ones. Droplet size from ground sprayer nozzles is dependent on the nozzle type, size, and spray pressure (Nuyttens et al., 2007) as well as spray formulation (Miller and Butler Ellis, 2000). In addition to these effects, airblast sprayers are also influenced by secondary atomization resulting from air shear (Hewitt, 1997). Sprays from agricultural aircraft are also impacted by air shear as a result of the airspeed of the aircraft, as well as the orientation angle of the nozzle with respect to the airstream (Bouse, 1994; Czaczyk, 2012). Kirk (2007) introduced a more efficient methodology for assessing spray droplet size for a given nozzle based on the effects of the four significant parameters: orifice size, spray pressure, orientation angle, and airspeed. Using a response surface methodology, specifically the experimental design proposed by Box and Behnken (1960), Kirk (2007) developed a series of models that allowed prediction of droplet size characteristics at any combination of the four parameters. These models have been well received by, and provide a significant benefit to, the agricultural aviation industry.

The models developed by Kirk (2007) incorporated 40° and 80° flat fans, #46 and #56 disc core tips, as well as several aerial-specific nozzles, including the CP-03, CP-09, and CP-11TT nozzles with straight stream tips (CP Products, Wichita Falls, Tex.). As noted by Kirk (2007), the CP-03 nozzle was not included as part of earlier Spray Drift Task Force (SDTF) studies but had increased from 5% to 60% usage by the aerial application industry at the time of Kirk's study. Since that time, a similar trend has occurred with a dedicated set of 20°, 40°, and 80° flat fans tips for the CP-11TT nozzle body, as well as the introduction of the CP-06 swivel, which allows for rapid orientation angle changes through a series of 15° indents. The CP-11TT nozzle body allows for placement of three individual tips of any fan angle or orifice size, providing applicators with quick, convenient nozzle changes. The 20° flat fan tip from CP Products is a recent product and has limited data reported. A nozzle similar to the CP-03, the Davidon Tri-Set (Davidon, Inc., Unadilla, Ga.), was introduced since that time and has been picked up within the industry. Although there is a current Tri-Set nozzle model, it was developed several years after the others, and as such its measurement methods are not as well documented.

The models developed by Kirk (2007) were some of the

Submitted for review in August 2014 as manuscript number MS 10896; approved for publication by the Machinery Systems Community of ASABE in January 2015.

Mention of company or trade names is for description only and does not imply endorsement by the USDA. The USDA is an equal opportunity provider and employer.

The authors are **Bradley K. Fritz, ASABE Member,** Agricultural Engineer, and **W. Clint Hoffmann,** Agricultural Engineer, USDA-ARS Aerial Application Technology Research Unit, College Station, Texas. **Corresponding author:** Bradley Fritz, 3103 F&B Road, College Station, TX 77845; phone: 979-255-0109; e-mail: brad.fritz@ars.usda.gov.

first aerial nozzle data points to have the droplet size tied to the ASABE droplet size classification (DSC) standard (ASABE, 2009). As this standard was primarily intended for the classification of ground sprayer nozzles, no recommended nozzles or method existed for classifying aerial nozzles. Kirk (2007) interpreted and applied the standard to aerial nozzles using droplet size data measured from the recommended reference nozzles operated in still air and spraying a water-only solution to set the size classification boundaries. Additionally, all aerial nozzles tested used water plus a non-ionic surfactant (Triton X-100, Dow Chemical, Midland, Mich.). Since this work, a series of spray nozzles and pressures have been recommended for use in aerial nozzle testing that provide equivalent droplet size statistics to those recommended by ANSI/ASAE Standard S572.1 (ASABE, 2009) but can be evaluated under the same measurement setup as the nozzles being evaluated, as intended by the standard (Hewitt, 2008). Efforts are currently in progress to revise the current standard to include these nozzles for all aerial nozzle evaluations.

The droplet size data used to develop the current aerial spray nozzle models were measured using a setup initially described by Bouse and Carlton (1985) that included an engine-driven centrifugal fan with a 30 cm × 30 cm square outlet and a PMS laser spectrometer system (OAP-2D-GAI probe, Particle Measurement Systems, Inc., Boulder, Colo.). Kirk's (2007) work positioned the PMS probe 0.74 m downstream of the nozzle orifice exit for all nozzles, except for the 0° deflection straight stream nozzles, which required moving the probe to 1.12 m downstream. Full plume scans were accomplished by a series of continuous horizontal scans traversing 1/8, 3/8, 5/8, and 7/8 of the plume height. Both the fan and the measurement system have since been upgraded with more modern technologies. The current setup has been used in a number of aerial spray sizing studies (Hoffmann et al., 2009; Fritz et al., 2010) and includes a blower system capable of airspeeds up to 98 m s^{-1} through a 30 cm square opening. Additionally, the PMS was replaced with a Sympatec HELOS laser diffraction instrument (Sympatec, Clausthal-Zellerfeld, Germany). As will be discussed later, a single scan is used versus the series of scans required by the PMS system.

As detailed by Kirk (2007), each nozzle was evaluated following a multi-factor experimental design that allowed for the development of a predictive model. The Box-Behnken design (BBD) response surface method (RSM) chosen resulted in 27 coded treatment points, which were different combinations of the minimum, maximum, and mid-points of each of the four parameters (orifice, pressure, orientation angle, and airspeed). One of the characteristics of the BBD is that there are no treatment points at the vertices of the space defined by the factors tested (SAS, 2014). In other words, the BBD does not require measurements of treatment combinations of more than two factors at their extremes (either minimum or maximum). This is beneficial when conducting treatments at these extreme points would be difficult or prohibitive, but it potentially results in a higher level of uncertainty in predictions at operational points where two or more factors are at their extreme settings. By contrast, a central composite design (CCD) includes a number of the combinations of factors at their extremes in the design that, while requiring a few additional treatment points, potentially enhances predictions at these extremes, which represent the edges of the response surface (Myers et al., 2009). Both the BBD and CCD assume that each factor tested is continuous such that the minimum, maximum, and mid-point are readily set during testing. As noted by Kirk (2007), this was not always the case for the nozzles tested. With both the CP-03 and CP-09 nozzles, the orifices (1.55, 1.98, 3.18, and 4.37 mm) are not evenly spaced such that the midpoint of the maximum and minimum (2.96 mm) is not available. Additionally, with the CP-09, the built-in deflection plates are 0°, 5°, and 30°, meaning the experimental model requires a mid-point of 15°. Kirk (2007) obtained custom-built nozzles from the manufacturer with the correct mid-point orifices, but it is unsure how the needed 15° deflector was dealt with. Similarly with a few of the other nozzles tested, an exact mid-point orifice was not available, so the closest available was selected (Kirk, 2007). This was an issue that had to be addressed as part of the current project. Within JMP software, a custom model design builder allows for efficient construction of an RSM design using a combination of continuous and discrete factors, which generates an *I*-optimal design within the operational region defined by the factors, thereby minimizing the average prediction variances (SAS, 2009). This allows for custom RSM designs that fit nozzles with non-continuous orifices sizes and/or deflection angles.

With the current fixed-wing nozzle models, airspeeds are limited to 71.5 m s^{-1} (160 mph) due to the maximum velocity that could be generated by the fan that was used. Today's modern, larger aircraft have cruising speeds up to 85 m s^{-1} (190 mph) and while typical application working speeds do not exceed 71.5 m s^{-1}, as agricultural production and crop production needs increase, future application speeds might well exceed these airspeeds. With the current testing facilities, this upper airspeed limit can be extended to accommodate future needs. Additionally, the current models limit spray pressure to 414 kPa (60 psi). Current work by the authors has demonstrated that atomization can be reduced at higher spray pressures, e.g., 621 kPa (90 psi), as a result of increasing the liquid exit velocity from the nozzle and reducing the differential velocity between the liquid and surrounding airstream. Increasing the current pressure limits with the new models will allow applicators an additional means of controlling droplet size. Finally, the current models limit the nozzle orientation angle on the CP-11TT and disc orifice straight stream tips to 20°. In the past several years, the authors have had requests from applicators and nozzle manufacturers for data at extended orientation angles.

In preparation for updating the fixed-wing nozzles models, extended efforts were made to standardize testing methods with other facilities conducting similar research. A series of atomization trials were conducted at the USDA-ARS facility (College Station, Tex.), the spray atomization research facility at the University of Queensland (Gatton, Queensland, Australia) and at the University of Nebraska-Lincoln (North Platte, Neb.) (Fritz et al., 2014). Each of the three facilities uses the same model of the Sympatec

HELOS system and has similar wind tunnel type setups for testing aerial spray nozzles. The standard methods reported were developed to prevent confounding data at similar treatment points from being reported by different laboratories. The methods reported as part of this article follow those developed as part of the three laboratory standardization work.

The objectives of this work were to update the current USDA-ARS aerial spray nozzle atomization models by using updated test methods and systems, to incorporate new nozzles and extended operational parameter ranges, and to provide DSC ratings with the aerial reference nozzles proposed by Hewitt (2008). As specified by Kirk (2007), these models must be easily usable by aerial applicators to determine the DSC from their operational setup to aid in meeting requirements set either by crop protection product labels or state regulatory agencies. The data presented will be incorporated into the USDA-ARS aerials sprays smartphone app, which is available for Apple (Cupertino, Cal.) and Google Play (Google, Mountain View, Cal.) compatible phones.

METHODS

Each nozzle was tested following a set of experimental designs as defined by the BBD, CCD, or custom response surface methods. For most nozzles, data were collected for both the BBD and CCD designs, as well as a number of additional points used to test the goodness of fit. The final response surface model was developed and compared, where nozzle types and settings overlapped, to the current nozzle models. DSCs between the current and new models were also compared. The final mathematical models were incorporated into a single spreadsheet with a simple front-end user interface requiring only inputs of nozzle type, orifice size, orientation angle, spray pressure, and operation airspeed in order to provide an estimate of droplet size characteristics and classification.

TESTING SETUP

All droplet size testing was conducted in the USDA-ARS Aerial Application Technology Research Unit's aerial nozzle testing facility. High-speed air was generated using a 164 kW diesel engine-driven forward-curve centrifugal fan (1.27 m diameter) with a tapered exit approximately 2.4 m long that exhausted through a 45 × 30 cm outlet. The tapered transition was equipped with a series of 2.5 cm diameter × 61 cm long tubes to straighten the airflow near the nozzle. Airspeed was controlled by varying the engine speed and was measured near the outlet section using a pitot tube and an aircraft airspeed indicator dial. The exit was fitted with a boom section mounted on a set of linear guides and fit to an electric linear traverse. The boom was plumbed such that the nozzle was positioned in the center (horizontally) of the wind tunnel exit (fig. 1). Pressure to the spray tank was controlled by a pressure regulator, and spray pressure at the nozzle was measured using an electronic pressure gauge (PX409-100GUSB, Omega Engineering, Stamford, Conn.) that was positioned within 20 cm (8 in) of the nozzle outlet.

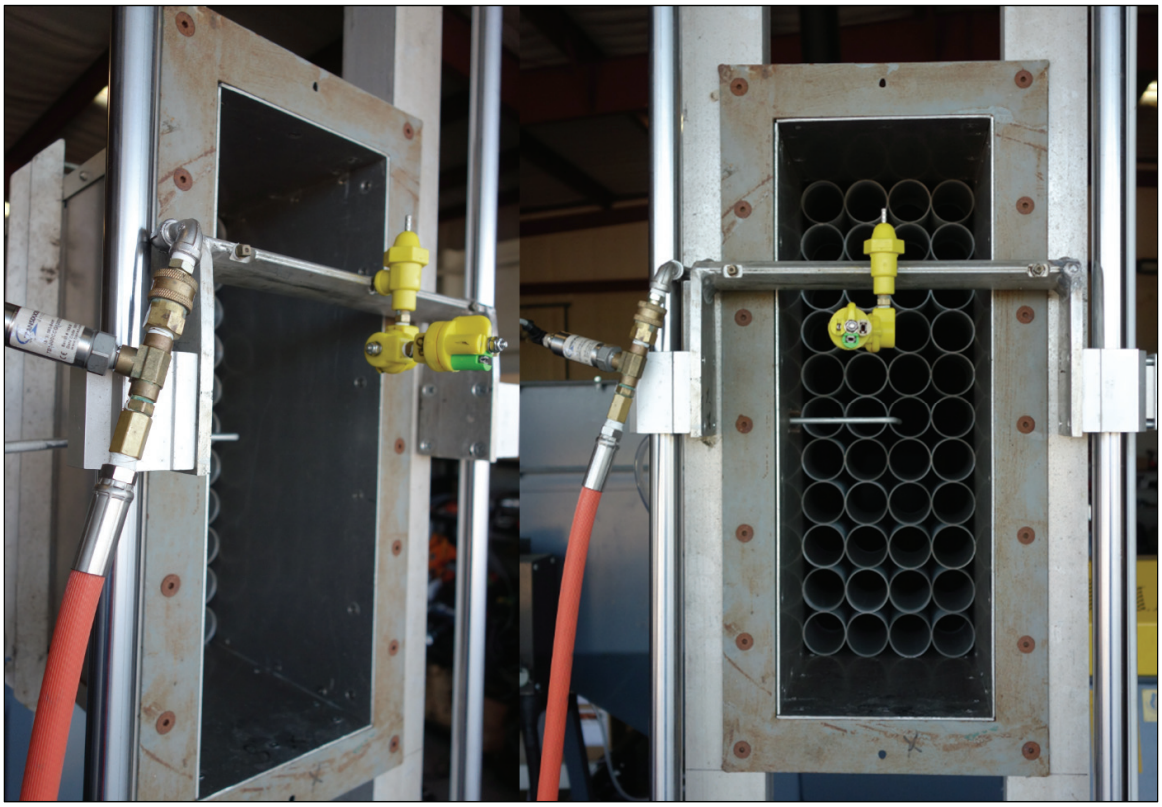

Figure 1. Side view (left) and front view (right) of aerial nozzle test facility tunnel outlet with CP-11TT 40° flat fan with CP-06 swivel mounted on airfoil boom and vertical linear traverse.

Droplet size data were measured using a Sympatec HELOS laser diffraction system. The majority of the testing was conducted using the R6 lens (0.5/9-1750 µm dynamic size range in 32 bins). However, a few of the nozzles and operational settings, specifically the straight stream nozzles at 0° orientation and the narrower angle flat fan nozzles at 621 kPa (90 psi) and 54 m s^{-1} (120 mph), required switching to the R7 lens (0.5/18-3500 µm). The Sympatec system was located 45.7 cm downwind stream of the nozzle and positioned such that the measurement zone was aligned vertically with the center of the tunnel outlet. The 0° orientation straight stream nozzle required moving the Sympatec system farther downstream, to 1.5 m, to ensure complete atomization of the spray. At this position, a 0.91 m square section was position between the nozzle and the Sympatec system to maintain the airstream and ensure spray movement through the measurement zone. Measurements at each treatment point consisted of a minimum of three replicated measurements, with additional replicates added if needed to ensure that standard deviations were within 10% of the means for each parameter reported. Each replicated measurement consisted of the nozzle being traversed vertically such that the entire spray plume was traversed through the measurement zone. The droplet size metrics recorded for model development included the $D_{V0.1}$, $D_{V0.5}$, and $D_{V0.9}$ (ASABE, 2012) as well as % <100 µm and % <200 µm (percent of spray volume comprised of droplets with diameters of less than 100 and 200 µm, respectively). Each treatment point was coded in the HELOS software with nozzle and operational setting information. Means for each set of replicates were calculated using JMP (SAS, 2014) and used to develop each specified model.

NOZZLES TESTED AND EXPERIMENTAL DESIGNS

A total of 12 nozzles were evaluated as part of this work. The 40° and 80° flat fan tips, CP-03, CP-09, and CP-11TT with straight stream tips, and disc orifice straight stream tips included in Kirk's (2007) testing were included. The #46 and #56 cores were replaced with a #45 core, and both stainless steel and ceramic disc core nozzles were tested. Additional nozzles included the 20°, 40°, and 80° flat fan tips in the CP-11TT nozzle body, as well as the Davidon Tri-Set nozzle. Data collection for all nozzles, except the CP-03, CP-09, and Davidon Tri-Set, included the treatment points needed for both the BBD and CCD designs, as well as an additional 8 to 10 independent data points (set at a combination of the four operational parameters that did not overlap the BBD and CCD treatment points) to be used in testing each model's fit. Experimental designs were developed in JMP using the maximum and minimum values of the effect variables (orifice, pressure, orientation, and airspeed). The response variables of interest that were coded into the designs were $D_{V0.1}$, $D_{V0.5}$, and $D_{V0.9}$, % <100 µm, and % <200 µm. With these inputs, the BBD or CCD designs were generated. For the CCD design, the axial points were set to fit the maximum and minimum ranges of the four factors. The custom designs for the other three nozzles were generated following a similar approach, with the exception that orifice was set as a discrete factor with each actual orifice size specified; for the CP-09, orientation was also entered as a discrete factor with each level entered. All nozzle models used spray pressure and airspeed as continuous factors with treatment levels (low, middle, and high) of 207, 414, and 621 kPa (30, 60, and 90 psi) and 54, 67, and 80 m s^{-1} (120, 150, and 180 mph), respectively. The orifice sizes and orientation angles for each of the nozzles tested are shown in table 1. The response surface models developed are also shown in table 1.

While Kirk (2002) provided a coded layout of the BBD design, the authors thought it worthwhile to do so again, along with the CCD design, to contrast the differences between the two (table 2). The custom designs used are also presented for comparison to the others. Where the BBD never has more than two factors at either extreme combined, by contrast the CCD has several treatments in which three or four factors are at maximum or minimum levels. The custom design follows a similar approach, but as two of the factors are at discrete levels and the model does not have to account for a continuous space, the experimental design is more efficient (19 treatments vs. 25 for the BBD and CCD).

In addition to the nozzles tested to develop the atomization models, reference nozzle data were required to provide the DSC ratings required for complying with many product labels and state regulatory policies. Kirk (2007) used the reference nozzles and operational settings recommended by ANSI/ASAE Standard S572.1 (ASABE, 2009) to set the boundaries between the different spray classifications where all reference nozzle sizing was conducted in still air. The intent of the standard was to provide a means of rela-

Table 1. Response surface models evaluated for each nozzle tested with orifice size and orientation angle factor levels used with each model.

Nozzles Tested	Models Evaluated[a]	Orifice Sizes[b]	Orientation Angles
CP-11TT with 20° flat fan tips	BB, CCD	4, 12, 20	0°, 45°, 90°
CP-11TT with 40° flat fan tips	BB, CCD	4, 15, 30	0°, 45°, 90°
CP-11TT with 80° flat fan tips	BB, CCD	2, 15, 25	0°, 45°, 90°
Spraying Systems 40° flat fan	BB, CCD	2, 15, 30	0°, 45°, 90°
Spraying Systems 80° flat fan	BB, CCD	2, 15, 30	0°, 45°, 90°
CP-11TT with straight stream tips	BB, CCD	6, 15, 25	0°, 22.5°, 45°
Steel disc orifice straight stream	BB, CCD	6, 15, 25	0°, 22.5°, 45°
Steel disc orifice #45 core	BB, CCD	2, 8, 16	0°, 45°, 90°
Ceramic disc orifice #45 core	BB, CCD	2, 6, 10	0°, 45°, 90°
CP-03	Custom	0.062, 0.078, 0.125, 0.172	30°, 60°, 90°
CP-09	Custom	0.062, 0.078, 0.125, 0.172	0°, 5°, 30°
Davidon Tri-Set	Custom	0.062, 0.078, 0.125	0°, 22.5°, 45°

[a] BB = Box-Behnken response surface design, and CCD = central composite response surface design.
[b] Orifice sizes are as specified by the manufacturer; therefore, no units are shown.

Table 2. Box-Behnken, central composite, and custom response surface experimental design treatment combinations.[a]

	Box-Behnken				Central Composite				Custom[b]			
Treatment	X_1	X_2	X_3	X_4	X_1	X_2	X_3	X_4	X_1	X_2	X_3	X_4
1	-1	-1	0	0	-1	-1	-1	-1	3	0	0	3
2	-1	1	0	0	-1	-1	-1	1	1	0	1	3
3	1	-1	0	0	-1	-1	1	-1	4	1	0	2
4	1	1	0	0	-1	-1	1	1	3	1	-1	1
5	0	0	-1	-1	-1	1	-1	-1	4	-1	1	3
6	0	0	-1	1	-1	1	-1	1	1	-1	1	1
7	0	0	1	-1	-1	1	1	-1	3	0	1	2
8	0	0	1	1	-1	1	1	1	1	-1	-1	3
9	-1	0	0	-1	1	-1	-1	-1	4	-1	0	1
10	-1	0	0	1	1	-1	-1	1	1	1	-1	3
11	1	0	0	-1	1	-1	1	-1	1	1	1	1
12	1	0	0	1	1	-1	1	1	2	0	0	2
13	0	-1	-1	0	1	1	-1	-1	3	1	1	3
14	0	-1	1	0	1	1	-1	1	3	-1	-1	2
15	0	1	-1	0	1	1	1	-1	4	0	-1	3
16	0	1	1	0	1	1	1	1	2	0	0	2
17	-1	0	-1	0	-1	0	0	0	1	0	-1	1
18	-1	0	1	0	1	0	0	0	4	0	1	1
19	1	0	-1	0	0	-1	0	0	2	0	0	2
20	1	0	1	0	0	1	0	0	-	-	-	-
21	0	-1	0	-1	0	0	-1	0	-	-	-	-
22	0	-1	0	1	0	0	1	0	-	-	-	-
23	0	1	0	-1	0	0	0	-1	-	-	-	-
24	0	1	0	1	0	0	0	1	-	-	-	-
25	0	0	0	0	0	0	0	0	-	-	-	-

[a] Factor levels represent the minimum (-1), mid-point (0), and maximum (1) levels for each factor: X_1 = orifice, X_2 = airspeed, X_3 = spray pressure, and X_4 = orientation angle.

[b] Custom design is shown for X_1 (orifice) at four discrete levels and for orientation angle (X_4) at three discrete levels. The same number of treatments was used for the custom design with X_1 at three discrete levels with slight modifications to the factor combinations used.

tive nozzle comparison, as it has long been recognized that different instrument, methods, and facilities will return different absolute numbers for identical nozzles and operational settings (ASABE, 2009). The current standard specifying still air does not provide a valid reference for nozzles evaluated under aerial conditions (Hewitt, 2008). To address this, Hewitt (2008) determined a set of nozzles and spray pressures that, when evaluated in an airstream of 51 m s^{-1} (115 mph), provide equivalent droplet size data ($D_{V0.1}$, $D_{V0.5}$, and $D_{V0.9}$) to the data generated from ground-based reference nozzles. The recommended nozzle and pressure combinations for each category are: VF/F (11001 at 450 kPa), F/M (8003 at 550 kPa), M/C (8005 at 300 kPa), C/VC (6515 at 400 kPa), and VC/XC (4015 at 280 kPa). These recommended nozzles and settings were used in this model update.

DATA ANALYSIS

All data analysis and model development were done using JMP. Once final models were developed, all treatment points collected for a given nozzle that were not used as part of the model development were used as test fit points. For example, to test the goodness of fit of the CCD model for the CP-11TT 20° flat fan nozzle, the eight independent test points collected as well as the data used to generate the BBD model were used to compare to model-predicted values for the operational conditions of each treatment. Model test fitting was conducted using Excel (Microsoft Corp., Redmond, Wash.) by plotting the measured values for each treatment to those predicted by the model. Comparison of the current models to the new models, where nozzles, orifices, and other parameters overlapped, was done using custom software programmed in FORTRAN (Fortran PowerStation 4.0, Microsoft 1994-1995) to calculate the percent differences between the $D_{V0.1}$, $D_{V0.5}$, and $D_{V0.9}$, % <100 µm, and % <200 µm for the current and new models at 0.45 m s^{-1} (1 mph) increments of airspeed, 6.9 kPa (1 psi) increments of spray pressure, and each orifice and spray angle shared by the current and new models. Additionally, the change in DSC from the current model was determined. Summary statistics were determined using JMP.

RESULTS

Similar to Kirk (2007), second-order response relationships were fitted following the format of equation 1 to the data collected for each nozzle and model type evaluated:

$$Y = A + BX_1 + CX_2 + DX_3 + EX_4 + FX_1X_2 + GX_1X_3 + HX_2X_3 + IX_1X_4 + JX_2X_4 + KX_3X_4 + LX_1^2 + MX_2^2 + NX_3^2 + OX_4^2 \quad (1)$$

where

Y = atomization parameter to be predicted based on input combination of X_1 through X_4 (i.e., $D_{V0.1}$, $D_{V0.5}$, etc.)

X_1 = (orifice size – C_{sub1}) / C_{div1} (unitless, specific orifice number for each nozzle)

X_2 = (airspeed – C_{sub2}) / C_{div2} (mph for model input user interface)

X_3 = (spray pressure – C_{sub3}) / C_{div3} (psi for model input user interface)

X_4 = (orientation angle – C_{sub4}) / C_{div4} (degrees for model input user interface)

C_{subi} = constant subtraction term used to adjust each X_i

from input value to a value between -1 and 1 (unitless and unique for each nozzle)

C_{divi} = constant dividend term used to adjust each X_i from input value to a value between -1 and 1 (unitless and unique for each nozzle)

A to O = constant coefficients for each term of the prediction expression (unitless and unique for each nozzle).

All model terms were developed using imperial units, as the majority of the users of these models are U.S. aerial applicators for whom mph and psi are the common units for airspeed and spray pressure, particularly in regard to the currently available spray nozzle models. It should also be noted that the models are only applicable across the minimum and maximum ranges tested for each parameter. With all nozzle models, similar to the results found by Kirk (2007), the linear terms were dominant, with airspeed and orientation being most significant ($\alpha = 0.05$). Typically, the airspeed by orientation term was the most significant cross-factor for each parameter in the models.

GOODNESS OF FIT

The response surface equations for the BB and CCD models for all of the models tested had high R^2 values ranging from 0.94 to 0.99 for all droplet size parameters ($D_{V0.1}$, $D_{V0.5}$, and $D_{V0.9}$, % <100 µm, and % <200 µm), signifying that the models resulted in excellent estimates of each of the parameters measured that were used to develop the models. When looking at each of the models fit to both the independently run treatment points as well as the other model treatment points not used for that specific model, overall R^2 values were lower. The R^2 for the $D_{V0.1}$ fits ranged from 0.87 to 0.96 for the BB models and from 0.90 to 0.97 for the CCD models. For the custom models, $D_{V0.1}$ fits ranged from 0.83 to 0.92. In all cases where both BBD and CCD models were evaluated, the CCD resulted in the highest R^2 to the $D_{V0.1}$ data. Similarly, the R^2 for the $D_{V0.5}$ fits ranged from 0.90 to 0.95 for the BBD models and from 0.93 to 0.98 for the CCD models, with the CCD fits being better in all cases. For the custom models, the $D_{V0.5}$ fits ranged from 0.81 to 0.92. The R^2 for the $D_{V0.9}$ fits ranged from 0.86 to 0.97 for the BBD models and from 0.89 to 0.97 for the CCD models, with the CCD fits being equal or better in all cases. For the custom models, the $D_{V0.9}$ fits ranged from 0.85 to 0.9. The R^2 values for the % <100 µm and % <200 µm data ranged from 0.91 to 0.99 for the BBD models and from 0.93 to 0.99 for the CCD models, with CCD resulting in equal or better fits in all cases. Custom model R^2 for the same data ranged from 0.95 to 0.97. Given that the CCD models provided equal, and in most cases better, fits than the BBD models, the CCD model experimental design was incorporated into the updated nozzle models for all nozzles, except those for which custom designs were used (CP-03, CP-09, and Davidon Tri-Set). The subtraction and dividend terms for each nozzle model are given in the Appendix (table A1), and the unique coefficients for each nozzle are provided in tables A2 through A13.

DSC REFERENCE NOZZLE DATA

Droplet size data for the aerial reference nozzles suggested by Hewitt (2008) are given in table 3, along with the values reported by Hewitt for these nozzles. There is very close agreement between the data generated as part of this work and the data presented by Hewitt (2008). Moreover, recent efforts by Fritz et al. (2014) resulted in means for these same nozzles and settings with few significant differences between the three participating laboratories. By contrast, the reference nozzle data used for DSC in the current nozzle models are given in table 4. While these data were not originally presented by Kirk (2007), they are attributed to that work. It is readily apparent that there are differences between the two sets of DSC data, with the current model data having larger overall volume mean diameters than the updated aerial reference nozzle data. A number of references have documented that PMS data collection consistently produces larger average droplet diameters than laser diffraction based instruments (Arnold, 1987, 1990; Dodge, 1987). Teske et al. (2002) concluded that the major differences between the PMS system and other laser diffraction systems were primarily sampling and operational differences. The differences seen between these data sets are consistent with the reported literature. Additionally, while Hewitt (2008) selected the nozzles and pressures to be used in a high-speed tunnel to match droplet size data as closely as possible with the ANSI/ASAE S572.1 reference nozzle data, given the differences in nozzle and wind tunnel conditions, differences were expected beyond those attributable to the measurement system.

Table 3. Droplet size data measured using the Hewitt (2008) recommended reference nozzles in a 51 m s^{-1} airstream with standard deviations. The droplet size data reported by Hewitt (2008) for the same nozzles and categories are shown in parentheses.

DSC	Nozzle	Pressure (kPa)	$D_{V0.1}$ (µm)	$D_{V0.5}$ (µm)	$D_{V0.9}$ (µm)
VF/F	11001	450	64.0 +0.9 (63)	142.3 +1.4 (138)	235.5 +1.9 (237)
F/M	8003	550	128.8 +0.6 (114)	267.6 +0.5 (255)	466.3 +4.6 (444)
M/C	8005	300	164.3 +0.7 (157)	335.1 +1.3 (341)	563.7 +4.5 (561)
C/VC	6515	400	218.5 +0.6 (209)	463.9 +0.5 (440)	789.2 +3.7 (786)
VC/XC	4015	280	236.8 +3.9 (242)	510.2 +7.0 (522)	903.6 +16.6 (831)

Table 4. Droplet size data used to rate DSC for current nozzle models (Kirk, 2007). Values are means plus one standard deviation.

DSC	Nozzle	Pressure (kPa)	$D_{V0.1}$ (µm)	$D_{V0.5}$ (µm)	$D_{V0.9}$ (µm)
VF/F	11001	450	82.3 +1.5	176.7 +5.5	294.7 +14.0
F/M	11003	300	140.3 +0.6	277.3 +2.5	489.0 +34.7
M/C	11006	200	155.3 +4.6	416.7 +11.9	811.3 +22.5
C/VC	8008	250	239.0 +4.6	517.0 +13.7	892.7 +35.9
VC/XC	6510	200	295.3 +3.8	637.3 +18.0	1243.7 +145.9

COMPARISON OF CURRENT MODEL RESULTS TO THE NEW MODEL RESULTS

Comparing the current versions of the models to the newly generated models becomes challenging given the sheer number of combinations of orifice, pressure, orientation, and airspeed at which each nozzle can potentially operate. For example, there are over 57,000 unique combinations for the 40° flat fan nozzle alone over the defined modeling space. As such, general observations across the entire operational space, as well as summaries across ranges of airspeeds, i.e., 54-58, 58-63, 63-67, and 67-72 m s^{-1} (120-130, 130-140, 40-150, and 150-160 mph), and pressures, i.e., 207-276, 276-345, and 435-414 kPa (30-40, 40-50, and 50-60 psi), and for each orifice and orientation angle were made for each nozzle and set of operational parameters for which the current and new models overlap. Summary statistics were made for overlapping ranges in airspeed of 53.6 to 71.5 m s^{-1} (120 to 160 mph in 1 mph increments) and in pressure of 207 to 414 kPa (30 to 60 psi in 1 psi increments). Summary comparisons were also made for all models with data grouped by current model DSC. To compare the current and new models, percent differences, expressed as [(current – new)/current] × 100, were determined for $D_{V0.1}$, $D_{V0.5}$, and $D_{V0.9}$, % <100 µm, and % <200 µm. Additionally, the average change in current DSC was determined across the ranges expressed earlier and for each orifice size and orientation angle. The differences that are discussed in detail below are an effect of the differences in droplet measurement systems and reference nozzles between the two modeling efforts, as well as the effect of the different types of response surface models used.

The percentages of the operational combinations within each DSC for the current and new models of each nozzle are shown in table 5. Table 5 is meant as a quick guide for applicators when making nozzle selections. For example, if a specific crop protection product label requires a coarse spray, an applicator would see that, for the 40° flat fan nozzle, only 1% of all possible combinations of airspeed, orifice, pressure, and orientation would be able to produce a coarse spray. However, if the CP-11TT straight stream nozzle were chosen, approximately 50% of all operational combinations would produce a coarse or higher DSC. This nozzle selection guide gives the applicator a much better chance of producing the desired droplet size with the applicator's aircraft. Table 5 also highlights the shifting of the DSC between the current and new models. A specific analysis of each nozzle is provided in the following sections.

Table 5. Droplet size classifications expressed as percentage of all operational combinations for nozzles and operational settings where current and new models overlap.

	Droplet Size Classification					
Nozzle and Model	VF	F	M	C	VC	XC
40° flat fan						
Current	32	41	26	<1	0	0
New	17	66	15	1	0	0
80° flat fan						
Current	73	22	5	0	0	0
New	33	67	1	0	0	0
CP-03						
Current	55	37	8	0	0	0
New	6	93	1	0	0	0
CP-09						
Current	5	31	61	3	0	0
New	4	58	28	9	1	<1
CP-11TT straight stream						
Current	0	3	80	17	0	0
New	0	17	33	37	6	7
Davidon Tri-Set						
Current	0	26	61	11	2	0
New	11	53	14	9	4	10
Disc core straight stream						
Current	2	29	54	14	<1	0
New	0	24	32	31	6	7

40° Flat Fan

The current and new models overlap for the standard 40° flat fan nozzle for orientation angles from 0° to 90° (comparison made in 15° increments) and orifice sizes of 4, 6, 8, 10, 12, 15, 20, and 30. Over the entire shared operational surface, the average $D_{V0.1}$, $D_{V0.5}$, and $D_{V0.9}$ values decreased in the new model by 2.6%, 15.8%, and 1.6%, respectively, while the average % <100 µm and % <200 µm increased by 105.7% and 115.4%, respectively. Of the operational points, 65% retained the same DSC, while 20.3% increased by one class and 14.7% decreased by one class. Very similar changes were seen within each of the three spray pressure ranges; however, very different trends were seen when examining the differences with respect to orientation angles and orifice sizes. Generally speaking, the smaller orifices (4 to 10) had overall increases in $D_{V0.1}$ in the new model, averaging 20% to 30%, with 20% average decrease in $D_{V0.5}$ and 7% to 12% average decrease in $D_{V0.9}$. The DSCs remained the same for 60% to 65% of the 4 to 10 orifice operational points, with 30% to 35% increasing by one class and only 1% to 12% dropping by one class. The larger orifices (12 to 30) had overall decreases in $D_{V0.1}$ (10% to 40%) and $D_{V0.5}$ (9% to 16%), with increased differences in $D_{V0.1}$ and decreased differences in $D_{V0.9}$ as orifice size increased. While 60% to 70% of the larger orifice DSCs remained the same, 30% to 35% of the points dropped by one DSC and 2% to 4% increased by one DSC, depending on the orifice size. Across the entire operational surface, 46% of the previously rated very fine (VF) sprays remained in the same class, with 54% increasing to a fine (F) spray. Of the current F sprays, 90% remained an F spray, while 5% dropped to a VF spray and 5% increased to a medium (M) spray. Of the current M sprays, 50% remained the same, while 46% dropped to an F spray and 4% increased to a coarse (C) spray. Of the current C sprays, 55% remained C, with 45% dropping to an M spray. As a perspective on these class changes, with the current model, 32% of the overlapping operational points are VF spray, 41% are F, 26% are M, and less than 1% are C. Across the overlapping points, with the new model, 17% of the points are VF, 66% are F, 15% are M, and 1% are C.

80° Flat Fan

Like the 40° flat fan, the current and new 80° flat fan models overlap for orientation angles from 0° to 90°. However orifice sizes only overlap for 2, 4, 6, 8, and 10. Over the entire operational surface, the average $D_{V0.1}$ values increased with the new model by 46%, and $D_{V0.5}$ and $D_{V0.9}$

decreased by 20% and 10%, respectively. Overall, the % <100 µm values changed very little (<1%), while the % <200 µm averaged increases of 75%. Of the current DSC, 55% remained the same while 41% increased by one class and 4% decreased by one class. The $D_{V0.5}$, $D_{V0.9}$, % <100 µm, and % <200 µm changes were consistent across the four airspeed ranges, while average increases in $D_{V0.1}$ ranged from 7% to 100%, with greater increases at higher airspeeds. Of the current VF sprays, 44% remained a VF spray, with 56% increasing to an F spray. All of the current F sprays remained F, while 82% of the current M sprays dropped to F sprays and 13% remained as M sprays. Over the entire operational surface, 73% of the current operational combinations are VF, 22% are F, and only 5% are M. By comparison, across the new model overlapping points, 33% are VF, 67% are F, and 1% are M.

CP-03

The current and new models overlap across all available orifice sizes (0.061, 0.078, 0.125, and 0.172) and deflector angles (30°, 60°, and 90°) as well as the established airspeed and pressure ranges for which these comparisons were made. Compared to the current model, average predicted $D_{V0.1}$ data from across the entire combination of operational factors with the new model increased by 41%, while $D_{V0.5}$ and $D_{V0.9}$ on averaged decreased by 4% and 2%, respectively. The % <100 µm decreased by 5%, while the % <200 µm increased by 42%. Of the current DSC, 42% remained the same, while 50% increased by one class and only 8% decreased by one class. The changes in droplet size parameters were similar for both the spray pressure ranges and orifice sizes. Across all 30° orientation operational setups, average $D_{V0.1}$ increased by 39%, while $D_{V0.5}$ remained equal and $D_{V0.9}$ decreased on average by 25%. Of the current VF sprays, 99% increased to F sprays, while 98% of current F sprays remained F with 2% increasing to M sprays. Of the current M sprays, 97% decreased to F sprays with 4% remaining M. Overall, 55% of the current model's operational combinations are VF, 37% are F, and 8% are M, while with the new model 6% are VF, 93% are F, and 1% are M.

CP-09

The current and new models overlap across all orifice sizes (0.062, 0.078, 0.125, and 0.172) and orientation angles (0°, 5°, and 30°). Across the complete overlapping surface, $D_{V0.1}$ and $D_{V0.5}$ decreased with the new model, on average, by 18% and 6%, respectively, while $D_{V0.9}$ increased by 7%. The % <100 µm increased, on average, by 21%, while the % <200 µm increased 60%. These changes were consistent for each airspeed and pressure range compared, as well as each orifice size. However, with deflection angle, $D_{V0.1}$ decreased by 3% for the 0° angle, while $D_{V0.5}$ and $D_{V0.9}$ increased by 22% and 33%, respectively, while % <100 µm decreased by 23% and % <100 µm increased by 15%. With the 5° deflector, $D_{V0.1}$ and $D_{V0.5}$ decreased in the new model by 17% and 8%, respectively, while $D_{V0.9}$ increased by 10% and % <100 µm and % <200 µm increased by 3% and 40%, respectively. At 30°, $D_{V0.1}$, $D_{V0.5}$, and $D_{V0.9}$ all decreased (35%, 33%, and 23%, respectively), while both % <100 µm and % <200 µm increased (84% and 126%, respectively). The overlapping operational points had 50% remaining at the same DSC, while less than 1% decreased by two classes, 34% decreased by one class, and 16% increased by one class. Of the current VF sprays, 29% remained in the VF class, with 71% increasing to an F spray. Of the current F sprays, 75% remained in the F class, with 9% dropping to VF and 16% increasing to M. Of the current M sprays, 38% remained in the same class, with 52% dropping to F and 11% increasing to C. Of the current C sprays, 76% remained C, with 3% dropping to F, 24% increasing to VC, and less than 1% increasing to XC. With the current model, 5% of the operational points are VF sprays, while 31% are F, 61% are M, and 3% are C. By contrast, with the new model, 4% are VF, 58% are F, 28% are M, 9% are C, 1% are VC, and less than 1% are XC.

CP-11TT Straight Stream

The current and new models overlap for orifice sizes 8, 10, 12, 15, 20, and 25 and orientation angles of 0° and 15°. On average, across the overlapping operational space compared, with the new model, $D_{V0.1}$ decreased by 24%, and $D_{V0.5}$ and $D_{V0.9}$ increased by 10% and 6%, respectively. Similar to the Davidon Tri-Set, the % <100 µm increased on average by a minimum of 100%, but predicted values for % <100 µm of less than 1%, or in many cases zero, resulted in inflated increase estimates. The % <200 µm predictions increased, on average, by more than 200%. These results were consistent across all factors except orientation angle. The 0° orientation angle showed similar results; however, at 15°, $D_{V0.1}$, $D_{V0.5}$, and $D_{V0.9}$ all decreased (31%, 6%, and 8%, respectively). Across the full overlapping surface, 41% of the current DSC remained in the same class, with 16% dropping by one class, 33% increasing by one class, and 10% increasing by two classes. Of the current VF sprays, 49% remained a VF spray, and 51% increased to an F spray. Of the current F sprays, 40% remained F, 20% dropped to VF, 36% increased to M, and 4% increased to C. Of the current M sprays, 52% remained M, 14% increased to C, and 34% increased to VC. With the current model, 3% of current operational setups result in F sprays, 80% result in M, and 17% result in C. With the new model, 17% are F, 33% are M, 37% are C, 6% are VC, and 7% are XC.

Davidon Tri-Set

The current and new models overlap across all available orifice sizes (0.062, 0.078, and 0.125) and deflector angles (0°, 22.5°, and 45°), as well as the established airspeed and pressure ranges of comparison. Across all operational combinations, the $D_{V0.1}$ values decreased with the new model on average by 36%, with $D_{V0.5}$ decreasing by 5% and $D_{V0.9}$ increasing by 2%. The % <100 µm increased on average by a minimum of 100%, but as the current model has quite a few points where the predicted % <100 µm is less than 1%, or in many cases zero, determining an actual average, without arbitrarily assigning a maximum percent difference cutoff point, was difficult. The % <200 µm predictions increased, on average, by more than 200%. These differences were consistent across airspeed and spray pressure

ranges, orientation angles, and orifice sizes. The DSC classification remained the same for 37% of the operational setting combinations, with 10% dropping by two classes, 30% dropping by one class, 13% increasing by one class, and 10% increasing by two classes. Across the entire overlapping operational surface, the current model has 26% of the sprays rated F, 61% rated M, 11% rated C, and 2% rated VC, while the new model has 11% rated VF, 53% rated F, 14% rated M, 9% rated C, 4% rated VC, and 10% rated XC.

Disc Core Straight Stream

The current and new models overlap at orientation angles of 0°, 10°, and 20° and orifice sizes of 6, 8, 10, and 12. Across this overlapping space, with the new model, $D_{V0.1}$, $D_{V0.5}$, and $D_{V0.9}$ all increased, on average, by 3%, 12%, and 18%, respectively, while % <100 µm decreased by 36% and % <200 µm increased by 16%. With respect to DSC, 46% remained in the same class, with 4% dropping by one class, 38% increasing by one class, and 12% increasing by two classes. While the $D_{V0.9}$ and % <100 µm changes were consistent across all factors compared, there were differences in $D_{V0.1}$, $D_{V0.5}$, and % <200 µm. At lower airspeeds, $D_{V0.1}$ decreased on average by 4%, with increases of 17% at the higher airspeed range. $D_{V0.5}$ followed previously mentioned change rates. At 0° and 10° deflection, the differences were similar to the overall trends, but at 20°, $D_{V0.1}$ and $D_{V0.5}$ decreased by 10% and 4%, respectively, while $D_{V0.9}$ increased by 5%. With respect to orifice size, $D_{V0.1}$ increased on average by 17% for the smallest orifices and decreased by 4% to 7% for the largest two orifices, while $D_{V0.5}$ and $D_{V0.9}$ increased by 11% and 17%, respectively, and % <100 µm decreased by 40%. The % <200 µm decreased by 3% for the smallest orifice and then trended toward continual increases, up to 40%, as orifice size increased. Over the complete overlapping surface, 46% of the DSC remained the same, with 4% dropping by one class, 38% increasing by one class, and 12% increasing by two classes. Of the current VF sprays, 80% increased to F, with 20% increasing to M. Of the current F sprays, 61% remained F, with 32% increasing to M and 9% increasing to C. Of the current M sprays, 43% remained M, with 7% dropping to F, 44% increasing to C, and 6% increasing to VC. Of the current C sprays, 36% remained C, with 23% increasing to VC and 41% increasing to XC. All (100%) of the current VC sprays remained VC. With the current model, 2% of the overlapping operational combinations are VF, 29% are F, 54% are M, 14% are C, and less than 1% are VC, while with the new model, 24% of the sprays are F, 32% are M, 31% are C, 6% are VC, and 7% are XC.

Characteristics of the New Models at Extended Pressures and Airspeeds

One of the primary reasons for these updates was to extend the spray pressure and airspeed ranges for all of the nozzles tested. As mentioned previously, as agricultural aircraft become larger and faster, there is a critical need for information on what happens to droplet size beyond the current 71.5 m s^{-1} (160 mph) limit and for tools to help mitigate the production of driftable fine droplets in the spray. These updated models show that an increase in spray pressure, at a constant airspeed, increases the overall droplet size spectra. As an example, a standard 40° flat fan nozzle (8 orifice) with a spray pressure of 207 kPa (30 psi) at 54 m s^{-1} (120 mph) results in an M spray with $D_{V0.1}$, $D_{V0.5}$, and % <100 µm of 160 µm, 349 µm, and 1.5%, respectively. Increasing the airspeed to 72 m s^{-1} (160 mph) results in an F spray with $D_{V0.1}$, $D_{V0.5}$, and % <100 µm of 115 µm, 295 µm, and 6.6%, respectively. Increasing the airspeed even more, to 80 m s^{-1} (180 mph), results in an F spray with $D_{V0.1}$, $D_{V0.5}$, and % <100 µm of 93 µm, 206 µm, and 11.9%, respectively. Using the same nozzle and airspeed and increasing the pressure to 621 kPa (90 psi) results in an F spray with $D_{V0.1}$, $D_{V0.5}$, and % <100 µm of 104 µm, 241 µm, and 8.8%, respectively. As these results show, while the decrease in droplet size due to increased airspeed does not see much relief with the increased spray pressure (likely due to the 40° fan angle, which has increased air shear on the outer edges of the fan), the increase is present.

With a straight stream nozzle, these results are more dramatic. Using a CP-11TT with straight stream tips, and using the same operational settings at 54 m s^{-1} (120 mph) results in an XC spray with $D_{V0.1}$, $D_{V0.5}$, and % <100 µm of 249 µm, 554 µm, and 1.7%, respectively. Increasing the airspeed to 72 m s^{-1} (160 mph) results in an M spray with $D_{V0.1}$, $D_{V0.5}$, and % <100 µm of 137 µm, 305 µm, and 5.9%, respectively. Increasing the airspeed to 80 m s^{-1} (180 mph) results in an F spray with $D_{V0.1}$, $D_{V0.5}$, and % <100 µm of 101 µm, 233 µm, and 9.3%, respectively. Using the same nozzle and airspeed and increasing the pressure to 621 kPa (90 psi) results in an M spray with $D_{V0.1}$, $D_{V0.5}$, and % <100 µm of 164 µm, 398 µm, and 4.8%, respectively. While adapting a typical agricultural aircraft to operate at 621 kPa may take some effort, as this model shows, in combination with a straight stream nozzle, an M spray, which is required by many product labels for application by air, can be obtained. It should be noted that this is not the only option for an M spray at 80 m s^{-1} (180 mph), merely one selected to illustrate the changes in droplet size occurring with changes in both airspeed and spray pressure.

Conclusions

The development of spray atomization models has proven to be a very useful tool for aerial applicators. Due to improvement in agricultural aircraft and in the scientific equipment and methods used for measuring spray droplet size, it was necessary to develop new models. The new models increase the usable ranges of airspeed, spray pressure, and nozzle orientation to better fit the needs and application conditions of modern aerial application. Different response surface methodologies that allow for a better fit of the modeled data to the measured data over the entire range of operational conditions were used in the development of the new models. By contrasting the new models with the current USDA-ARS spray atomization models developed by Kirk (2007), the following conclusions can be drawn:

- The new models use a central composite design (CCD), which resulted in a better of goodness of fit

between the modeled data and measured data than the Box-Behnken design (BBD) that the current models use.
- The CP-03, CP-09, and Davidon Tri-Set models use a custom model design that better accommodates the non-uniform spread of orifice sizes and orientation angles, which do not fit the format required for the CCD or BBD.
- While detailed descriptions of the changes in droplet size parameters for each nozzle are provided in the text, the new models generally tended to group droplet size classifications (DSCs) around the fine and medium categories and less in the very fine category, as compared to the current models for flat fans and disc core nozzles, with the opposite trend seen for straight stream nozzles.
- The new models show that as airspeed increases across the total operational span, the droplet size spectra for all nozzles decrease. The models also show that higher spray pressures, at the same airspeed, dramatically increase spray droplet size and can be used to counteract the increased atomization seen when operating at higher airspeeds.

REFERENCES

Arnold, A. C. (1987). The drop size of the spray from agricultural fan spray atomizers as determined by a Malvern and the Particle Measuring System (PMS) instrument. *Atomization Spray Tech., 3*(1), 155-167.

Arnold, A. C. (1990). A comparative study of drop sizing equipment for agricultural fan-spray atomizers. *Aeronaut. Sci. Tech., 12*(2), 431-445. http://dx.doi.org/10.1080/02786829008959358.

ASABE. (2009). S572.1: Spray nozzle classification by droplet spectra. St. Joseph, Mich.: ASABE.

ASABE. (2012). S327.3: Terminology and definitions for agricultural chemical application. St. Joseph, Mich.: ASABE.

Bouse, L. F. (1994). Effect of nozzle type and operation on spray droplet size. *Trans. ASAE, 37*(5), 1389-1400. http://dx.doi.org/10.13031/2013.28219.

Bouse, L. F., & Carlton, J. B. (1985). Factors affecting size distribution of vegetable oil spray droplets. *Trans. ASAE, 28*(4), 1068-1073. http://dx.doi.org/10.13031/2013.32389.

Box, G. E., & Behnken, D. W. (1960). Some new three-level designs for the study of quantitative variables. *Technometrics, 2*(4), 455-475. http://dx.doi.org/10.1080/00401706.1960.10489912.

Czaczyk, Z. (2012). Influence of air flow dynamics on droplet size in conditions of air-assisted sprayers. *Atomization and Sprays, 22*(4), 275-282. http://dx.doi.org/10.1615/AtomizSpr.2012003788.

Dodge, L. G. (1987). Comparison of performance of drop-sizing instruments. *Appl. Optics, 26*(7), 1328-1341. http://dx.doi.org/10.1364/AO.26.001328.

Fritz, B. K., Hoffmann, W. C., & Bagley, W. E. (2010). Effects of spray mixtures on droplet size under aerial application conditions and implications on drift. *Appl. Eng. Agric., 26*(1), 21-29. http://dx.doi.org/10.13031/2013.29467.

Fritz, B. K., Hoffmann, W. C., Kruger, G. R., Henry, R. S., Hewitt, A., & Czaczyk, Z. (2014). Comparison of drop size data from ground and aerial nozzles at three testing laboratories. *Atomization and Sprays, 24*(2), 181-192. http://dx.doi.org/10.1615/AtomizSpr.2013009668.

Hewitt, A. J. (1997). Droplet size and agricultural spraying, Part 1: Atomization, spray transport, deposition, drift, and droplet size measurement techniques. *Atomization and Sprays, 7*(3), 235-244. http://dx.doi.org/10.1615/AtomizSpr.v7.i3.10.

Hewitt, A. J. (2008). Droplet size spectra classification categories in aerial application scenarios. *Crop Protection, 27*(9), 1284-1288. http://dx.doi.org/10.1016/j.cropro.2008.03.010.

Hoffmann, W. C., Fritz, B. K., & Lan, Y. (2009). Evaluation of a proposed drift reduction technology high-speed wind tunnel testing protocol. *J. ASTM Intl., 6*(4), 1-10. http://dx.doi.org/10.1520/JAI102122.

Kirk, I. W. (2002). Measurement and prediction of helicopter spray nozzle atomization. *Trans. ASAE, 45*(1), 27-37. http://dx.doi.org/10.13031/2013.7866.

Kirk, I. W. (2007). Measurement and prediction of atomization parameters from fixed-wing aircraft spray nozzles. *Trans. ASABE, 50*(3), 693-703. http://dx.doi.org/10.13031/2013.23123.

Miller, P. C., & Butler Ellis, M. C. (2000). Effects of formulation on spray nozzle performance for applications from ground-based boom sprayers. *Crop Protection, 19*(8-10), 609-615. http://dx.doi.org/10.1016/S0261-2194(00)00080-6.

Myers, R. H., Montgomery, D. C., & Anderson-Cook, C. M. (2009). *Response Surface Methodology: Process and Product Optimization Using Designed Experiments* (3rd ed.). Hoboken, N.J.: John Wiley and Sons.

Nuyttens, D., Baetens, K., De Schampheleire, M., & Sonck, B. (2007). Effect of nozzle type, size, and pressure on spray droplet characteristics. *Biosys. Eng., 97*(3), 333-345. http://dx.doi.org/10.1016/j.biosystemseng.2007.03.001.

SAS. (2009). *JMP 8 Design and Experiments Guide* (2nd ed.). Cary, N.C.: SAS Institute, Inc.

SAS. (2014). JMP online documentation: Response surface designs. Cary, N.C.: SAS Institute, Inc. Retrieved from www.jmp.com/support/help/Response_Surface_Designs.shtml.

Teske, M. E., Thistle, H. W., Hewitt, A. J., & Kirk, I. W. (2002). Conversion of droplet size distributions from PMS optical array probe to Malvern laser diffraction. *Atomization and Sprays, 12*(1-3), 267-281. http://dx.doi.org/10.1615/AtomizSpr.v12.i123.140.

APPENDIX

Table A1. Subtraction and division terms (eq. 1) used to convert factor inputs to model coded inputs (-1 to 1).

	X_1 (Orifice size, unitless)		X_2 (Airspeed, mph)		X_3 (Pressure, psi)		X_4 (Orientation, degrees)	
Nozzle	C_{sub1}	C_{div1}	C_{sub2}	C_{div2}	C_{sub3}	C_{div3}	C_{sub4}	C_{div4}
CP-11TT 20° flat fan	12	8	150	30	60	30	45	45
CP-11TT 40° flat fan	17	13	150	30	60	30	45	45
CP-11TT 80° flat fan	16	14	150	30	60	30	45	45
CP-03	0.1165	0.0555	150	30	60	30	60	30
Steel disc core #45	9	7	150	30	60	30	45	45
Ceramic disc core #45	6	4	150	30	60	30	45	45
Standard 40° flat fan	16	14	150	30	60	30	45	45
Standard 80° flat fan	16	14	150	30	60	30	45	45
CP-09	0.117	0.055	150	30	60	30	15	15
CP-11TT straight stream	15.5	9.5	150	30	60	30	22.5	22.5
Disc core straight stream	7	5	150	30	60	30	22.5	22.5
Davidon Tri-Set	0.0935	0.0315	150	30	60	30	22.5	22.5

Table A2. CP-11TT 20° flat fan nozzle model coefficients.

Droplet Size Parameters	Coefficient Terms				
	Intercept	X_1	X_2	X_3	X_4
$D_{V0.1}$	87.4949	14.5056	-28.4556	6.2889	-49.2500
$D_{V0.5}$	217.3831	34.1222	-62.2111	12.2000	-104.9611
$D_{V0.9}$	382.3559	85.5500	-115.9389	26.0000	-213.8278
% <100 µm	12.8298	-3.4459	6.0169	0.4988	11.7652
% <200 µm	44.2475	-6.6833	12.7722	-0.6611	26.1667
	$X_1 \times X_2$	$X_1 \times X_3$	$X_2 \times X_3$	$X_1 \times X_4$	$X_2 \times X_4$
$D_{V0.1}$	-6.1125	3.3125	1.9125	-4.5500	14.6000
$D_{V0.5}$	-16.7000	8.9875	1.5375	-17.7000	35.7750
$D_{V0.9}$	-28.0375	15.4250	0.5000	-52.4875	67.0375
% <100 µm	-0.5896	-0.5198	0.0324	-2.4668	2.8744
% <200 µm	0.3500	-0.1000	-2.2625	-2.1000	1.0375
	$X_3 \times X_4$	X_1^2	X_2^2	X_3^2	X_4^2
$D_{V0.1}$	-6.1250	-4.8274	4.8226	0.9226	15.6726
$D_{V0.5}$	-20.7375	-6.3469	13.2531	1.2531	28.4031
$D_{V0.9}$	-43.6000	-6.3653	27.8347	5.1847	63.4347
% <100 µm	1.8527	1.8307	0.0907	-0.3193	2.9382
% <200 µm	3.8625	2.8613	-0.4387	-1.0387	3.0113

Table A3. CP-11TT 40° flat fan nozzle model coefficients.

Droplet Size Parameters	Coefficient Terms				
	Intercept	X_1	X_2	X_3	X_4
$D_{V0.1}$	82.8487	9.8471	-24.8931	2.0625	-42.5419
$D_{V0.5}$	208.4340	30.9614	-57.6972	6.0939	-93.1330
$D_{V0.9}$	368.0412	82.7236	-106.5266	17.9592	-189.7160
% <100 µm	14.3059	-3.8233	6.3481	1.2594	12.8495
% <200 µm	49.0928	-6.6528	12.9750	0.8417	25.9673
	$X_1 \times X_2$	$X_1 \times X_3$	$X_2 \times X_3$	$X_1 \times X_4$	$X_2 \times X_4$
$D_{V0.1}$	-5.9810	3.2891	-0.0596	-3.6190	16.8896
$D_{V0.5}$	-16.7114	9.1007	-0.3490	-13.4784	33.7882
$D_{V0.9}$	-30.6977	21.6246	-8.8622	-48.8614	60.5230
% <100 µm	-1.0968	0.0294	-0.2446	-3.0901	2.2644
% <200 µm	0.3919	0.3909	-2.7031	-2.6175	-0.8757
	$X_3 \times X_4$	X_1^2	X_2^2	X_3^2	X_4^2
$D_{V0.1}$	-7.7539	-7.5747	3.0292	0.2364	16.8765
$D_{V0.5}$	-18.1422	-20.3663	10.1757	-1.9591	35.3847
$D_{V0.9}$	-41.8411	-38.3028	27.1283	-5.0211	79.4328
% <100 µm	2.3896	3.3023	0.3208	-0.3579	2.4260
% <200 µm	4.0473	6.8748	-0.2693	-1.0418	-1.8306

Table A4. CP-11TT 80° flat fan nozzle model coefficients.

Droplet Size Parameters	Coefficient Terms				
	Intercept	X_1	X_2	X_3	X_4
$D_{V0.1}$	80.3911	15.3801	-19.1401	0.0057	-24.7577
$D_{V0.5}$	198.7351	40.9078	-41.1522	0.2703	-53.5934
$D_{V0.9}$	345.2431	87.8584	-66.2710	3.2716	-110.8328
% <100 µm	16.1105	-6.6487	7.8178	0.5550	9.9480
% <200 µm	52.9832	-13.3000	13.2802	0.7957	18.0747
	$X_1 \times X_2$	$X_1 \times X_3$	$X_2 \times X_3$	$X_1 \times X_4$	$X_2 \times X_4$
$D_{V0.1}$	-7.0297	1.7830	0.3823	-8.5850	7.8309
$D_{V0.5}$	-16.1245	4.8201	2.9198	-21.8673	13.4514
$D_{V0.9}$	-23.3256	11.5979	12.2104	-52.5524	19.3814
% <100 µm	-1.5263	-0.3843	0.2859	-1.6520	2.6523
% <200 µm	1.7081	-1.2385	-2.2938	3.1121	-0.2313
	$X_3 \times X_4$	X_1^2	X_2^2	X_3^2	X_4^2
$D_{V0.1}$	-2.3822	-13.0232	2.7540	-0.8015	9.3967
$D_{V0.5}$	-4.9291	-29.7470	5.9512	-2.7308	17.8526
$D_{V0.9}$	-15.2276	-55.8081	8.0831	-9.3177	48.9498
% <100 µm	1.0362	6.4252	-0.3628	-1.2423	1.7484
% <200 µm	1.5313	12.1010	-0.9107	-1.3607	-0.4607

Table A5. CP-03 nozzle model coefficients.

Droplet Size Parameters	Coefficient Terms				
	Intercept	X_1	X_2	X_3	X_4
$D_{V0.1}$	85.3017	6.1833	-22.5002	-0.8752	-13.0544
$D_{V0.5}$	202.2981	20.4833	-49.9783	0.4173	-29.3269
$D_{V0.9}$	354.9948	53.2556	-88.1306	4.5990	-77.1530
% <100 µm	13.5186	-2.2643	7.1100	0.0487	4.8440
% <200 µm	49.5756	-7.0716	17.3278	0.2628	11.6290
	$X_1 \times X_2$	$X_1 \times X_3$	$X_2 \times X_3$	$X_1 \times X_4$	$X_2 \times X_4$
$D_{V0.1}$	-2.9289	0.5038	2.2875	3.8489	1.0500
$D_{V0.5}$	-8.7866	4.5359	3.4938	8.1082	1.2813
$D_{V0.9}$	-12.2372	4.9547	-0.8063	3.1150	5.3313
% <100 µm	-0.5492	-0.1951	-0.6251	-1.7063	2.0568
% <200 µm	0.4875	-1.2545	-1.7074	-3.5538	2.6788
	$X_3 \times X_4$	X_1^2	X_2^2	X_3^2	X_4^2
$D_{V0.1}$	2.2000	-1.5703	3.9195	-0.5305	0.3695
$D_{V0.5}$	5.3813	-6.9933	9.0336	-0.9664	6.1836
$D_{V0.9}$	4.9063	-8.9682	17.0359	1.0359	14.1859
% <100 µm	0.1903	0.7462	0.8345	0.1810	1.1660
% <200 µm	0.0629	3.1776	0.1006	-0.4043	0.4207

Table A6. Steel disc core #45 nozzle model coefficients.

Droplet Size Parameters	Coefficient Terms				
	Intercept	X_1	X_2	X_3	X_4
$D_{V0.1}$	71.0799	6.4083	-17.7778	-0.9842	-8.4958
$D_{V0.5}$	179.4539	23.3016	-35.5582	-2.0272	-18.6902
$D_{V0.9}$	350.5049	54.7634	-63.1450	-0.3905	-21.3941
% <100 µm	18.2467	-5.5254	10.4625	0.5944	6.5838
% <200 µm	57.4757	-10.6167	14.4230	0.4331	7.2042
	$X_1 \times X_2$	$X_1 \times X_3$	$X_2 \times X_3$	$X_1 \times X_4$	$X_2 \times X_4$
$D_{V0.1}$	-4.1465	0.8324	1.1640	0.3771	-1.0905
$D_{V0.5}$	-11.8213	-0.5539	3.4291	3.7223	-0.2894
$D_{V0.9}$	-23.7092	-0.5156	5.0489	18.2123	2.3434
% <100 µm	-1.0026	-0.3910	-0.6343	-3.2761	3.9250
% <200 µm	4.6003	0.3381	-1.9188	-2.8863	-1.0688
	$X_3 \times X_4$	X_1^2	X_2^2	X_3^2	X_4^2
$D_{V0.1}$	-1.5370	-2.4765	3.6690	-0.6723	-3.4718
$D_{V0.5}$	-2.1974	-14.5659	4.3920	-0.8980	-8.3191
$D_{V0.9}$	-2.6417	-34.5221	8.2468	3.8306	-44.7582
% <100 µm	1.3770	3.1593	1.5167	0.1879	3.0440
% <200 µm	1.1438	7.6828	-0.6907	0.4093	4.6093

Table A7. Ceramic disc core #45 nozzle model coefficients.

Droplet Size Parameters	Coefficient Terms				
	Intercept	X_1	X_2	X_3	X_4
$D_{V0.1}$	71.1847	10.0618	-17.1703	0.8224	-12.4890
$D_{V0.5}$	176.9451	27.3514	-37.0359	1.7993	-27.8294
$D_{V0.9}$	333.1581	57.9618	-69.9943	7.7274	-47.5442
% <100 µm	18.9443	-6.7523	10.1951	-1.7730	8.4181
% <200 µm	59.4780	-11.0667	14.8889	-0.9278	11.1111
	$X_1 \times X_2$	$X_1 \times X_3$	$X_2 \times X_3$	$X_1 \times X_4$	$X_2 \times X_4$
$D_{V0.1}$	-6.5179	-1.7288	1.8057	-1.5969	1.0688
$D_{V0.5}$	-13.5128	-3.0334	4.5241	-3.7213	1.5207
$D_{V0.9}$	-29.8930	1.2961	6.4149	-4.0899	4.5011
% <100 µm	-1.2179	1.4037	-0.9645	-2.9625	4.4679
% <200 µm	4.8375	0.4500	-2.1875	0.0250	0.2375
	$X_3 \times X_4$	X_1^2	X_2^2	X_3^2	X_4^2
$D_{V0.1}$	0.8397	-1.4562	3.1030	-2.1967	0.3670
$D_{V0.5}$	1.3641	-10.7186	4.0173	-3.9906	-0.3657
$D_{V0.9}$	1.0617	-26.8615	9.0126	0.0108	-27.2035
% <100 µm	-1.1247	2.7165	1.6514	0.6135	1.6507
% <200 µm	0.3750	5.6090	-0.1910	1.3590	2.0090

Table A8. Standard 40° flat fan nozzle model coefficients.

Droplet Size Parameters	Coefficient Terms				
	Intercept	X_1	X_2	X_3	X_4
$D_{V0.1}$	85.6050	9.5838	-22.1611	-0.5675	-38.6737
$D_{V0.5}$	223.0998	39.6139	-52.0487	2.7982	-80.8006
$D_{V0.9}$	401.7905	95.0661	-86.9949	13.9648	-165.1396
% <100 µm	12.9816	-5.8333	8.0024	0.3476	14.1939
% <200 µm	45.4911	-9.6485	13.0354	0.3733	23.7331
	$X_1 \times X_2$	$X_1 \times X_3$	$X_2 \times X_3$	$X_1 \times X_4$	$X_2 \times X_4$
$D_{V0.1}$	-6.5189	2.0607	4.1763	-1.1108	10.9603
$D_{V0.5}$	-18.2936	3.1661	6.7145	-11.7949	20.8692
$D_{V0.9}$	-23.7840	8.1268	14.5744	-41.6656	32.2290
% <100 µm	-1.9008	0.3702	-0.4366	-5.6234	4.3429
% <200 µm	1.5179	0.4403	-3.2948	-3.1405	-0.4623
	$X_3 \times X_4$	X_1^2	X_2^2	X_3^2	X_4^2
$D_{V0.1}$	-2.9472	-6.7162	0.1304	-2.8351	14.2789
$D_{V0.5}$	-9.8552	-27.7919	3.3160	-7.1113	24.2098
$D_{V0.9}$	-31.8123	-53.4737	0.5432	-6.8031	60.2964
% <100 µm	1.2064	3.4956	2.0858	0.8585	2.6107
% <200 µm	2.9422	8.1139	1.1967	-1.0915	1.0251

Table A9. Standard 80° flat fan nozzle model coefficients.

Droplet Size Parameters	Coefficient Terms				
	Intercept	X_1	X_2	X_3	X_4
$D_{V0.1}$	80.8321	9.1462	-17.1935	-1.6631	-29.1637
$D_{V0.5}$	206.7940	36.0787	-40.2681	-2.2977	-60.0826
$D_{V0.9}$	370.7755	83.1137	-67.9946	-0.9735	-124.2546
% <100 µm	14.7532	-5.9854	8.0092	0.8413	13.3174
% <200 µm	50.4298	-10.9958	12.1480	1.5038	20.6535
	$X_1 \times X_2$	$X_1 \times X_3$	$X_2 \times X_3$	$X_1 \times X_4$	$X_2 \times X_4$
$D_{V0.1}$	-6.2031	1.1153	2.2330	-3.0050	7.0658
$D_{V0.5}$	-15.1531	2.6013	6.3498	-13.8201	12.0695
$D_{V0.9}$	-21.6655	4.6599	14.2166	-42.0886	18.6074
% <100 µm	-1.5615	-0.3971	-0.0430	-4.4047	3.9478
% <200 µm	2.1091	0.0059	-3.5839	0.6085	-0.5183
	$X_3 \times X_4$	X_1^2	X_2^2	X_3^2	X_4^2
$D_{V0.1}$	-1.6830	-6.3633	0.9181	-4.6214	7.9518
$D_{V0.5}$	-4.9170	-27.6193	5.3175	-8.3008	12.7407
$D_{V0.9}$	-15.7443	-60.1549	13.0084	-18.2223	37.0027
% <100 µm	1.1571	4.0675	1.5792	1.2885	2.4198
% <200 µm	2.0324	10.4491	-0.0160	-0.1226	1.0435

Table A10. CP-09 nozzle model coefficients.

Droplet Size Parameters	Coefficient Terms				
	Intercept	X_1	X_2	X_3	X_4
$D_{V0.1}$	62.2759	-5.0616	-41.3849	11.4612	-37.4518
$D_{V0.5}$	109.2070	-10.9466	-112.5253	44.3979	-114.8313
$D_{V0.9}$	300.8848	25.4515	-214.0947	94.4398	-208.9857
% <100 µm	10.9364	-0.7405	5.4778	-0.2540	4.1396
% <200 µm	41.0699	-3.4073	16.2845	-2.1455	13.2469
	$X_1 \times X_2$	$X_1 \times X_3$	$X_2 \times X_3$	$X_1 \times X_4$	$X_2 \times X_4$
$D_{V0.1}$	4.9438	-11.3916	-13.5102	10.8326	14.0342
$D_{V0.5}$	18.0409	-38.1078	-48.8317	27.6676	41.8002
$D_{V0.9}$	21.5472	-56.6161	-122.7420	36.3935	69.8678
% <100 µm	-0.0335	-0.3283	0.1671	-1.4334	0.9587
% <200 µm	-0.7468	-0.5425	0.5523	-4.6798	2.4997
	$X_3 \times X_4$	X_1^2	X_2^2	X_3^2	X_4^2
$D_{V0.1}$	-10.2401	-2.7581	14.0445	3.5972	54.3854
$D_{V0.5}$	-32.8022	-12.3607	43.6482	13.7889	190.5735
$D_{V0.9}$	-55.2960	18.6384	91.2341	52.8274	199.7446
% <100 µm	0.3367	-0.1901	1.2461	0.0551	-1.8566
% <200 µm	0.3968	0.3070	1.9499	-1.1857	-7.1517

Table A11. CP-11TT straight stream nozzle model coefficients.

Droplet Size Parameters	Coefficient Terms				
	Intercept	X_1	X_2	X_3	X_4
$D_{V0.1}$	119.4535	-10.1872	-54.7197	21.5085	-52.8923
$D_{V0.5}$	291.0904	-14.8728	-127.5481	59.5501	-123.6877
$D_{V0.9}$	568.6660	-9.1869	-233.8423	126.4276	-240.1379
% <100 µm	6.7955	0.1698	5.3291	-1.1335	4.7547
% <200 µm	26.3551	0.2020	15.2494	-3.7685	13.9681
	$X_1 \times X_2$	$X_1 \times X_3$	$X_2 \times X_3$	$X_1 \times X_4$	$X_2 \times X_4$
$D_{V0.1}$	3.4273	-1.8292	-12.0883	14.6150	28.3362
$D_{V0.5}$	7.4343	-8.5687	-37.5109	27.6523	64.7024
$D_{V0.9}$	2.8396	-23.4533	-90.1549	48.1711	112.0114
% <100 µm	0.1866	0.1514	-0.4967	-1.1366	1.8709
% <200 µm	0.0580	0.3734	-0.9998	-3.1554	3.5761
	$X_3 \times X_4$	X_1^2	X_2^2	X_3^2	X_4^2
$D_{V0.1}$	-20.2415	3.7448	15.7868	0.9818	7.3041
$D_{V0.5}$	-53.6263	7.1775	39.1187	2.8444	18.8152
$D_{V0.9}$	-117.5258	28.2184	92.3359	-2.6694	-2.3928
% <100 µm	0.5040	-0.1437	0.9768	0.2842	1.5700
% <200 µm	1.8836	-0.5098	1.6994	0.7769	2.9733

Table A12. Disc core straight stream nozzle model coefficients.

Droplet Size Parameters	Coefficient Terms				
	Intercept	X_1	X_2	X_3	X_4
$D_{V0.1}$	127.1902	-13.2551	-57.6130	17.3427	-56.9436
$D_{V0.5}$	316.8280	-18.5167	-131.2386	46.8677	-123.7916
$D_{V0.9}$	635.7534	12.3147	-246.1203	112.5647	-228.9846
% <100 µm	6.1291	-0.2872	5.4576	-0.8864	4.8855
% <200 µm	24.0286	-0.4348	15.3364	-3.3142	14.0175
	$X_1 \times X_2$	$X_1 \times X_3$	$X_2 \times X_3$	$X_1 \times X_4$	$X_2 \times X_4$
$D_{V0.1}$	6.3486	-3.4020	-9.1232	23.8405	33.3496
$D_{V0.5}$	11.7241	-9.7310	-26.8683	39.6215	68.3374
$D_{V0.9}$	12.0349	-10.6156	-76.5128	44.0849	127.3541
% <100 µm	0.3241	0.2543	-0.3302	-2.0006	1.5153
% <200 µm	0.4764	1.0032	-0.9986	-5.0462	2.6460
	$X_3 \times X_4$	X_1^2	X_2^2	X_3^2	X_4^2
$D_{V0.1}$	-16.2674	-16.0818	16.3050	2.3867	17.4202
$D_{V0.5}$	-39.4591	-34.7703	37.8759	1.0887	34.0364
$D_{V0.9}$	-102.1506	-69.1006	72.2824	13.5266	19.0394
% <100 µm	0.4485	2.0753	0.7755	-0.0016	1.0792
% <200 µm	1.1995	5.4332	1.2742	0.1732	1.0819

Table A13. Davidon Tri-Set nozzle model coefficients.

Droplet Size Parameters	Coefficient Terms				
	Intercept	X_1	X_2	X_3	X_4
$D_{V0.1}$	102.5435	-7.7112	-58.0160	26.9446	-67.5103
$D_{V0.5}$	242.7426	-4.4283	-134.3129	74.3681	-167.4649
$D_{V0.9}$	451.5393	12.2106	-216.9586	133.8671	-307.6643
% <100 µm	8.9159	0.7068	5.2315	-0.8393	6.2734
% <200 µm	35.2548	0.5352	15.6989	-3.7031	19.6826
	$X_1 \times X_2$	$X_1 \times X_3$	$X_2 \times X_3$	$X_1 \times X_4$	$X_2 \times X_4$
$D_{V0.1}$	-0.9860	20.2018	-18.1157	4.3087	45.4093
$D_{V0.5}$	-8.1497	55.8518	-47.4177	5.6829	105.0998
$D_{V0.9}$	-9.4468	90.7375	-79.0649	-3.3835	162.5248
% <100 µm	0.2247	0.6277	-0.3884	-0.1147	1.4307
% <200 µm	-0.1788	1.5892	-1.2559	-1.4867	2.8964
	$X_3 \times X_4$	X_1^2	X_2^2	X_3^2	X_4^2
$D_{V0.1}$	-30.8049	2.7623	13.1017	-0.3206	30.5679
$D_{V0.5}$	-82.3799	-3.7092	30.6210	2.6141	92.3036
$D_{V0.9}$	-144.6834	-16.0963	53.0577	-0.4292	151.8336
% <100 µm	0.9432	0.8017	0.5720	-0.2825	0.6325
% <200 µm	2.5799	2.7756	0.0955	-0.4437	-2.0068